Theor. Comput. Fluid Dyn. (2010) 24:395–401
DOI 10.1007/s00162-009-0136-3

ORIGINAL ARTICLE

Valery L. Okulov · Jens N. Sørensen

Applications of 2D helical vortex dynamics

Received: 19 January 2009 / Accepted: 24 June 2009 / Published online: 24 July 2009

Abstract In the paper, we show how the assumption of helical symmetry in the context of 2D helical vortices can be exploited to analyse and to model various cases of rotating flows. From theory, examples of three basic applications of 2D dynamics of helical vortices embedded in flows with helical symmetry of the vorticity field are addressed. These included some of the problems related to vortex breakdown, instability of far wakes behind rotors and vortex theory of ideal rotors.

Keywords Helical vortices · Vortex breakdown · Instability of far wakes · Vortex theory of rotors

PACS 47.32.C

1 Introduction

In contrast to the equations governing helical Beltrami flows with colinear velocity and vorticity fields [1], the class of 2D helical vortex flows introduced in [2] is characterized by a simple linear correlation between axial w_z and azimuthal w_φ velocity components. This relation simply states that $w_z + r w_\varphi / l = const$, where $2\pi l$ is the pitch of the helical symmetry of the vorticity field and r is the radial distance from the symmetry axis. The primary assumption of the 2D theory has been carefully tested in swirling flows generated by different kinds of swirlers and vortex generators and for a wide range of operating conditions in, e.g. vortex devises [3], wakes behind rotors [4] and in the boundary layer downstream of a wall-mounted vortex generator [5].

The theory of 2D helical vortex dynamics is developing fast. At present, the fundamentals are based on various analytical components, which holds true for all values of the helix pitch such as (i) the 2D Biot–Savart law for helical filaments represented by Kapteyn series [6] or in a form with singularity separation [2]; (ii) solutions of helical vortex tubes with finite core, governed by series expansion of helical multipoles [7]; (iii) relations between the induction of vortex filaments and the self-induced velocity of helical vortex tubes [8] resulting in a closed analytical solution of the helix motion [9]; (iv) analytical representation of Goldstein's solution for the circulation of a helical vortex sheet in equilibrium [10]; (v) Kelvin's N-gon stability problem of point vortices generalized to multiple helical vortices [9,11]. In the following, we will show three examples of how the theory can be exploited to explain various features of helical flows: a simple model explaining vortex breakdown, a study of the instability of the far wake behind rotors, and some new results on the theory of ideal rotors (propellers or wind turbines). The main goal of the current work is to demonstrate the possibilities of using the concept of helical symmetry and attract attention the thriving theory.

Communicated by H. Aref

V. L. Okulov (✉) · J. N. Sørensen
Department of Mechanical Engineering and Center for Fluid Dynamics, Technical University of Denmark,
2800 Lyngby, Denmark
E-mail: vaok@mek.dtu.dk
E-mail: jnso@mek.dtu.dk

2 Control volume analysis of vortex breakdown

The phenomenon of vortex breakdown has being observed in numerous studies of slender vortices in pipe flows with high swirl (see, e.g. [12,13]). A chronological list of most of the theories can be found in [14]. In the following, we will describe a simple control volume (CV) analysis of vortex breakdown in pipe flows, in which helical symmetry is utilized to predict the velocity profiles behind the breakdown zone.

Vortex breakdown is characterized by two specific features: (1) a change in a flow topology; (2) a change in axial velocity from a jet-like profile before breakdown to a wake-like profile after breakdown. The second feature permits to study vortex breakdown as a change in helical symmetry of the vorticity field. For analyzing experimental data in connection with vortex breakdown, the following empirical relations are widely used [15]:

$$w_\varphi = \frac{K}{r}(1-\exp(-\alpha r^2)) \equiv \frac{\Gamma f(r,\varepsilon)}{2\pi r}; \quad w_z = W_1 + W_2\exp(-\alpha r^2) \equiv U - \frac{\Gamma f(r,\varepsilon)}{2\pi r} \tag{1}$$

where K, W_1, W_2 and α are empirical constants, with the following physical interpretation: circulation $\Gamma = 2\pi K$; helical pitch $l = K/W_2$; advection velocity $U = W_1 + W_2$; effective radius of vortex core $\varepsilon = 1/\sqrt{\alpha}$ and $f(r,\varepsilon) = 1-\exp(-r^2/\varepsilon^2)$ [16]. In this interpretation, the columnar vortex (1) has everywhere a dense distribution of helical filaments in the core (Fig. 1). The jet- and wake-like velocity profiles may be explained as flows induced by a right-handed helical vortex (with a "positive" pitch) or a left-handed helical vortex (with a "negative" pitch). The ability to induce reverse flow by the left-handed helical vortex explains the first breakdown property—the flow topology change.

Good correlations between measured velocity profiles and the axisymmetric solution (1), established in [15], permit to apply the CV analysis to study the flow. We do not take into account the influence of friction and flux losses on the pipe-wall. The CV consideration leads to conservation of five characteristic quantities [16,17]: flow rate Q, velocity circulation Γ, axial flux of angular momentum L, axial flux of momentum S and axial flux of energy E, This leads to the following relationship valid at the outflow of the pipe cross-section

$$\{Q,\Gamma,L,J,E\} = \{Q_0,\Gamma_0,L_0,J_0,E_0\} \tag{2}$$

with the right part is defined by the flow parameters before breakdown at the inflow pipe cross-section. Substitution of the expressions (1) in the left part of (2) allows to write a system of five non-linear algebraic equations for the parameters $\Gamma, l, \varepsilon, U$ of the vortex structure (1) and the static pressure p_∞ in the pipe.

Using algebraic manipulations to eliminate Γ, l, U and p_∞, the equation system (2) reduces to a non-linear energy equation than only depends on the vortex core radius ε:

$$U(\varepsilon)\left(-Q_0\frac{U(\varepsilon)}{2}+J_0+\frac{k_2(\varepsilon)}{2}\left(\frac{\Gamma_0}{l(\varepsilon)}\right)^2+k_4(\varepsilon)\Gamma_0\right)-\frac{\Gamma_0}{l(\varepsilon)}\left(k_1(\varepsilon)p_\infty(\varepsilon)+k_6(\varepsilon)\left(\frac{\Gamma_0}{l(\varepsilon)}\right)^2+k_5(\varepsilon)\Gamma_0^2\right)=E_0 \tag{3}$$

where $\Gamma = \Gamma_0$; $l(\varepsilon) = \Gamma_0^2\frac{k_1^2(\varepsilon)-\pi k_2(\varepsilon)}{\pi L_0-Q_0\Gamma_0 k_1(\varepsilon)}$; $U(\varepsilon) = \frac{L_0k_1(\varepsilon)-Q_0\Gamma_0k_2(\varepsilon)}{\Gamma_0(k_1^2(\varepsilon)-\pi k_2(\varepsilon))}$; and $p_\infty(\varepsilon) = \frac{J_0}{\pi} - \frac{1}{\pi}[U(\varepsilon)Q_0 - \frac{L_0}{l(\varepsilon)} + k_3(\varepsilon)\Gamma_0^2]$ are functions of ε only; and k_i are defined by integrals of $f(r,\varepsilon)$,

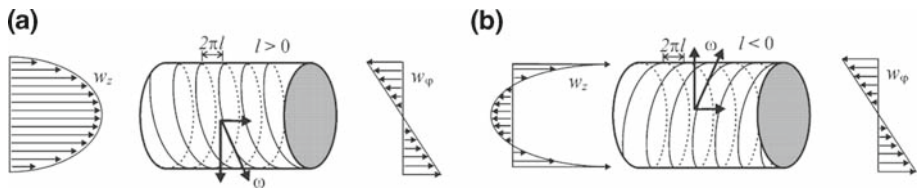

Fig. 1 Velocity profiles induced by vortex structures with different symmetry of vortex lines: **a** right-handed helical vortex and **b** left-handed helical vortex

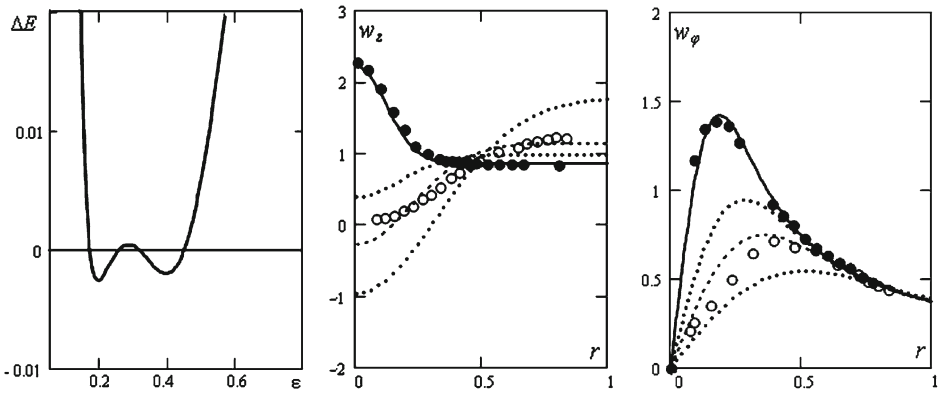

Fig. 2 Root of (3) and distributions of axial w_z and swirl w_φ velocities: *points* and *circles* are the experimental data from [9]; *lines* are result of the modeling (*solid* before vortex breakdown and *doted* after breakdown)

$$k_0(\varepsilon) = f(1,\varepsilon), \quad k_1(\varepsilon) = 2\pi \int_0^1 f(r,\varepsilon) r \mathrm{d}r, \quad k_3(\varepsilon) = 2\pi \int_0^1 \left(\int_0^r \frac{f^2(\sigma,\varepsilon)}{\sigma^3} d\sigma \right) r \mathrm{d}r,$$

$$k_2(\varepsilon) = 2\pi \int_0^1 f^2(r,\varepsilon) r \mathrm{d}r, \quad k_4(\varepsilon) = \pi \int_0^1 \frac{f^2(r,\varepsilon)}{r} \mathrm{d}r, \quad k_6(\varepsilon) = \pi \int_0^1 f^3(r,\varepsilon) r \mathrm{d}r,$$

$$k_5(\varepsilon) = \pi \int_0^1 \frac{f^3(r,\varepsilon)}{r} \mathrm{d}r + 2\pi \int_0^1 \left(\int_0^r \frac{f^2(\sigma,\varepsilon)}{\sigma^3} d\sigma \right) f(r,\varepsilon) r \mathrm{d}r.$$

The non-linear equation (3) has several roots in the full range of ε which makes possible the existence of several vortices with corresponding Γ, l, U, p_∞ to this roots and different helical symmetry under the same integral flow characteristics in the outflow cross-section (Fig. 2). The existence of a set of roots explains the possibility of the existence of several flow regimes at the same flow parameters undergoing a transition from a right handed to a left handed vortex structure, which is the experimental evidence of vortex breakdown [15]. Indeed the first root of (3) corresponds to a right-handed helical vortex with positive l and defines the initial flow in the inflow of the pipe cross-section with a jet-like axial velocity profile (seen as solid lines in Fig. 2 which are directly identical to experimental data [15]—points). The other roots correspond to left-handed helical vortices with negative values of l and wake-like axial velocity profiles (seen as dotted lines in Fig. 2 with a good correlation between one of them and the experimental data behind the breakdown zone [15]—circles).

Thus, explaining vortex breakdown as a transition in helical symmetry from a right-handed to a left-handed helical vortex has been supported by this simple CV-analysis of the experimental data [15]. Further evidence for this explanation can be found in numerical simulations [18].

3 Stability of tip vortex in far wake behind rotor

In 1912, Joukowski [19] proposed a simple model for a two-bladed propeller that basically consists of two rotating horseshoe vortices, corresponding to the tip and root vortices created by the rotation of the propeller with two blades. Corresponding to this, a far wake model of an N-blades rotor may be introduced as infinitely long N-helical vortices of strength Γ with constant pitch and radius, and a root or hub vortex represented by an infinitely long axial hub vortex of strength $\Gamma_0 = -N\Gamma$ (see the sketch in Fig. 3). Assuming a first-order perturbation of the position of the k-helical vortex of the form, $\delta \mathbf{r}_k = \delta \tilde{\mathbf{r}}_k \exp(\alpha t + 2\pi i k s/N)$, where $\delta \tilde{\mathbf{r}}_k$ is the amplitude vector of the perturbations, s is the sub-harmonic wave number that takes values within the range

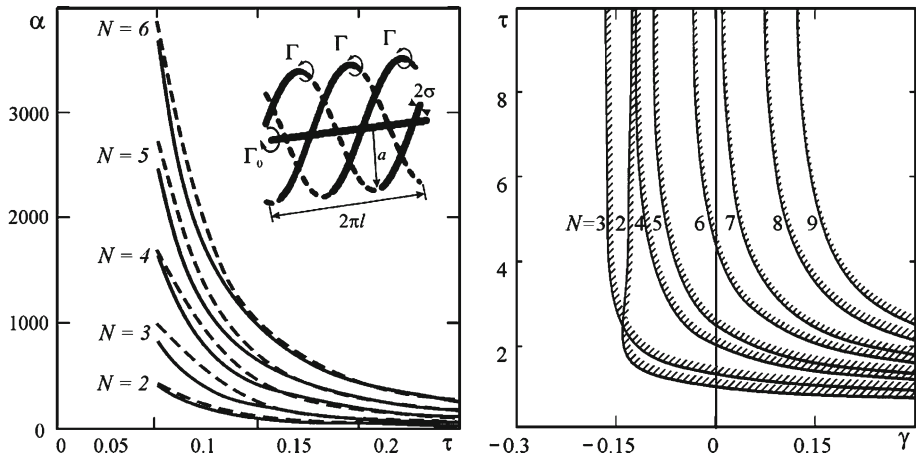

Fig. 3 *Left* Comparison of maximum amplification rate for $\gamma = 0$ (*solidlines* calculated by analytical solution (4) and *dashedlines* by numerical simulation of [14]). *Right* Neutral stability curves for helical tip vortices modeled far wake behind N-blade rotor as function of the circulation ratio γ (stable regions are located on the *dashedside* of the curve)

$[1, N-1]$, corresponding to $N-1$ independent eigenfunctions, and α is the amplification rate. An analysis of the stability [9,11] leads to the following analytical solution for the non-dimensional amplification rate

$$\alpha(4\pi a^2/\Gamma) = \sqrt{AB}, \tag{4}$$

where

$$A = s(N-s)\frac{\sqrt{1+\tau^2}}{\tau} - \frac{\tau}{4}\frac{4\tau^2-3}{(1+\tau^2)^{5/2}}\left(\frac{N}{s} - E - \psi\left(-\frac{s}{N}\right)\right);$$

$$B = -4N\gamma + s(N-s)\frac{(1+\tau^2)^{3/2}}{\tau^3} - 2N + 2\frac{N-2}{\tau^2} + \frac{1+2\tau^2}{\tau(1+\tau^2)^{1/2}}$$
$$+\frac{1}{\tau(1+\tau^2)^{3/2}}\left[\left(\tau^2-\frac{1}{4}\right)\left(E + \psi\left(-\frac{s}{N}\right) - \frac{N}{s} + \frac{3}{4} - 2\tau^2 - \ln\left(N\delta\frac{\left(1+\tau^2\right)^{3/2}}{\tau}\right)\right)\right]$$
$$+\frac{\tau^3}{(1+\tau^2)^{9/2}}\left(2\tau^4 - 6\tau^2 + \frac{3}{4}\right)\frac{\varsigma(3)}{N^2};$$

and $\varepsilon = \sigma/a$ is the dimensionless core size, $\tau = l/a$ is the dimensionless pitch, $\gamma = \Gamma_0/N\Gamma$ is the circulation ratio, $E = 0.577215\ldots$ is the Euler constant, $\varsigma(3) = 1.20206\ldots$ is the Riemann zeta function, and $\psi(\cdot)$ is the psi function. The value $\gamma = -1$ corresponds to Joukowski's far wake model. The first term of B describes the effect of the hub vortex. The vortex system is unstable if $AB \geq 0$ for any combination of $s, \tau, \varepsilon, \gamma$.

As an illustration of (4), in Fig. 3, we plot the absolute maximum amplification rate as function of helical pitch and number of tip vortices N for a far wake model without hub vortex ($\gamma = 0$). In the plot, results from our analytical model are compared to the numerical calculations by [20] which are a generalization of the single vortex theory [21]. The right plot of Fig. 3 shows neutral stability curves of the most unstable modes, when $\alpha(N, s^*, \gamma, \tau) = 0$, for different N-plets as function of the circulation ratio γ and helical pitch τ. From the data we can conclude that for $N < 7$ stable states may exist for $0 > \gamma > -1$, but for the important case $\gamma = -1$, where the total circulation of the vortex configuration is zero, the far wake described by the model of Joukowski is unconditionally unstable for all pitch values.

Most experiments on rotor wakes, by means of flow visualizations as well as numerical simulations [20,22], support this conclusion. But some investigations, however, indicate that the wake under some conditions may be stable. The review [23] shows examples from the pertinent literature on visualizations of stable vortex behavior.

An explanation for this apparent contradiction is that the model of Joukowski is too simple to describe the general behavior of rotor flows. Indeed, Joukowski's model is based on the assumption that the circulation is

constant over the blade span, and that the wake only consists of a hub vortex and trailing tip vortices. Considering the non-constant circulation that usually characterizes the operating range of a rotor, trailing vortices are created behind the rotor blades. These vortices form helical vortex sheets or screw surfaces along with the tip vortices. As it was shown in the experiments of [24], a visualization of this wake seemed to be stable on a long distance behind the rotor plane, whereas it clearly became unstable when the roll-up process of the vortex sheet formed concentrated tip vortices like in Joukowski's model.

4 Maximum power of wind turbines with finite number of blades

The determination of the ideal or theoretical maximum efficiency of a wind turbine rotor is today still a subject that has not been completely clarified. The most important upper limit was nearly a century ago derived by Betz [25] who, using axial momentum theory, showed that no more than 59% of the kinetic energy contained in a stream tube having same cross area as the rotor can be converted into useful work. Using general momentum theory Glauert [26] developed a model for the optimum rotor that included rotational velocities. In this approach, the rotor is treated as a rotating actuator disk, corresponding to a rotor with an infinite number of blades, and the maximum efficiency was shown to be a function of tip speed ratio, with values ranging from zero efficiency at zero tip speed ratio to the aforementioned 59% at high tip speed ratios. For a more realistic rotor with a finite number of blades, there have been many numerical or approximate models to determine the optimum rotor performance (see e.g. [27,28]). Using an analytical approach Betz [29] showed that the ideal efficiency is obtained when the distribution of circulation along the blade produces a rigidly moving helicoid wake that moves backward (in the case of a propeller) or forward (in the case of a wind turbine) in the direction of its axis with a constant velocity.

Based on the criterion of Betz, a theory for lightly loaded propellers was developed by Goldstein [10] using infinite series of Bessel functions. The theory was later generalized by Theodorsen [30] to cover cases of heavily loaded propellers. Paradoxically, in his analysis, Theodorsen correctly used the unsteady Bernoulli equation but neglected the time-dependent term in the momentum equation. Our interest in the subject was stimulated by the recent paper by Wald [31], who developed a complete set of Theodorsen's equations for determining the properties of an optimum heavily loaded propeller. However, when we tried to use the equations to analyze the optimum behavior of a wind turbine the theory always predicted a much lower efficiency than expected and what is known from experiments. Further, when extending the theory to the case of a rotor with infinitely many blades, the results did not comply with Betz limit and the general momentum theory.

Based on the analytical solution to the induction of helical vortex filament developed recently by Okulov [2,9], we analyzed in detail the original formulation of Goldstein [10] and found that the model by a simple modification could be extended to handle heavily loaded rotors in a way that is in full accordance with the general momentum theory [32]. Figure 4 presents the optimum power coefficient and corresponding thrust coefficient as a function of tip speed ratio for different number of blades. From the figures, it is evident that the optimum power coefficient has a strong dependency on the number of blades.

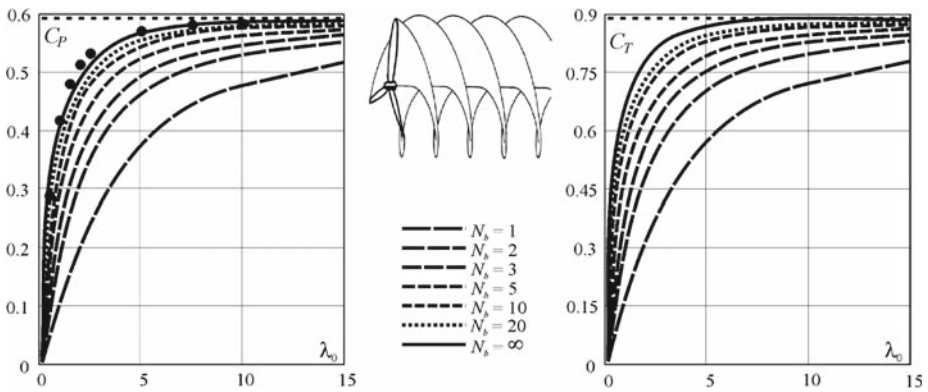

Fig. 4 Power coefficient, C_P, and thrust coefficient, C_T, as function of tip speed ratio for different number of blades of an optimum rotor. *Horizontal dashed lines* original Betz limit; *points* general momentum theory; *dashed and solid lines* present theory

The curves in Fig. 4 are compared to C_P-values obtained from the general momentum theory. The comparison shows that the results from the present theory for a rotor with infinite many blades are in excellent agreement with the values computed from general momentum theory.

5 Conclusions

Three applications of 2D dynamics of helical vortices embedded in flows with helical symmetry of the vorticity field have been considered. The applications include a novel explanation of vortex breakdown, a stability analysis of wakes behind rotors, and a solution to the problem of the optimum rotor with a finite number of blades. The main findings of the analysis can be summarized as follows:

1. The hypothesis that the change in axial velocity from a jet-like profile to a wake-like profile during vortex breakdown is associated with a transition in helical symmetry of the vortex structure has been supported by a control volume analysis of a swirling flow in a pipe.
2. An analytical solution to the stability problem of an infinitesimal spatial displacement of a multiple of N helical vortices with a hub vorticity distribution has been found. The solution allows us to provide an efficient analysis of some of the experimentally observed stable vortex arrays in the far wake behind wind turbines.
3. An analytical method to determine the loading on an optimum wind turbine rotor has been developed. The method, which basically is a modification to the original model of Goldstein, is based on an analytical solution to the helical wake vortex problem. The model enables to determine the optimum circulation distribution and the theoretical maximum efficiency of rotors with an arbitrary number of blades at all operating conditions.

References

1. Dritschel, D.G.: Generalized helical Beltrami flows in hydrodynamics and magneto hydrodynamics. J. Fluid Mech. **222**, 525–541 (1991)
2. Okulov, V.L.: Determination of the velocity field induced by vortex filaments of cylindric and weak conic shapes. Russ. J. Eng. Thermophys. **5**(2), 63–75 (1995)
3. Alekseenko, S.V., Kuibin, P.A., Okulov, V.L., Shtork, S.I.: Helical vortices in swirl flow. J. Fluid Mech. **382**, 195–243 (1999)
4. Troldborg, N.: Actuator Line Modelling of Wind Turbine Wakes. PhD thesis, Technical University of Denmark (2008)
5. Velte, C.M., Hansen, M.O.L., Okulov, V.L.: Helical structure of longitudinal vortices embedded in turbulent wall-bounded flow. J. Fluid Mech. **619**, 167–177 (2009)
6. Hardin, J.C.: The velocity field induced by a helical vortex filament. Phys. Fluids **25**, 1949–1952 (1982)
7. Fukumoto, Y., Okulov, V.L.: The velocity field induced by a helical vortex tube. Phys. Fluids **17**(10), 107101(1–19) (2005)
8. Boersma, J., Wood, D.H.: On the self-induced motion of a helical vortex. J. Fluid Mech. **384**, 263–280 (1999)
9. Okulov, V.L.: On the stability of multiple helical vortices. J. Fluid Mech. **521**, 319–342 (2004)
10. Goldstein, S.: On the vortex theory of screw propellers. Proc. R. Soc. Lond. A **123**(792), 440–465 (1929)
11. Okulov, V.L., Sørensen, J.N.: Stability of helical tip vortices in a rotor far wake. J. Fluid Mech. **576**, 1–25 (2007)
12. Hall, M.G.: Vortex breakdown. Annu. Rev. Fluid Mech. **4**, 195–218 (1972)
13. Leibovich, S.: The structure of vortex breakdown. Annu. Rev. Fluid Mech. **10**, 221–246 (1978)
14. Lucca-Negro, O., O'Doherty, T.: Vortex breakdown: a review. Prog. Energy Combust. Sci. **27**(4), 431–481 (2001)
15. Garg, A.K., Leibovich, S.: Spectral characteristics of vortex breakdown flow fields. Phys. Fluids **22**, 2053–2964 (1979)
16. Okulov, V.L.: The transition from the right helical symmetry to the left symmetry during vortex breakdown. Tech. Phys. Lett. **22**(10), 798–800 (1996)
17. Murakhtina, T., Okulov, V.: Changes in topology and symmetry of vorticity field during the turbulent vortex breakdown. Tech. Phys. Lett. **26**(10), 432–435 (2000)
18. Okulov, V.L., Sørensen, J.N., Voigt, L.K.: Vortex scenario and bubble generation in a cylindrical cavity with rotating top and bottom. Eur. J. Mech. B **24**(1), 137–148 (2005)
19. Joukowski, N.E.: Vortex theory of a propeller screw. Trudy Otdeleniya Fizicheskikh Nauk Obshchestva Lyubitelei Estestvoznaniya **16**, 1 (1912) (in Russian)
20. Gupta, B.P., Loewy, R.G.: Theoretical analysis of the aerodynamic stability of multiple, interdigitated helical vortices. AIAA J. **12**(10), 1381–1387 (1974)
21. Widnall, S.E.: The stability of a helical vortex filament. J. Fluid Mech. **54**, 641–663 (1972)
22. Bhagwat, M.J., Leishman, J.G.: Stability analysis of helicopter rotor wakes in axial flight. J. Am. Helicopter Ass. **45**, 165–178 (2000)
23. Vermeer, L.J., Sorensen, J.N., Crespo, A.: Wind Turbine Wake Aerodynamics. Prog. Aerosp. Sci. **39**, 467–510 (2003)
24. Felli, M., Guj, G., Camussi, R.: Effect of the number of blades on propeller wake evolution. Exp. Fluids **44**, 409–418 (2008)
25. Betz, A.: Das Maximum der theoretisch möglichen Ausnützung des Windes durch Windmotoren. Zeitschrift für Das Gesamte Turbinenwesen **26**, 307–309 (1920)

26. Glauert, H.: Airplane propellers. In: Durand, W.F. (ed.) Division in Aerodynamic Theory, vol. IV, pp. 169–360. Springer, Berlin (1935)
27. Chattot, J.-J.: Optimization of wind turbines using helicoidal vortex model. Trans. ASME **125**, 418–424 (2003)
28. Wood, D.H., Boersma, J.: On the motion of multiple helical vortices. J. Fluid Mech. **447**, 149–171 (2001)
29. Betz, A.: Schraubenpropeller mit Geringstem Energieverlust, Dissertation, Gottingen Nachrichten, Gottingen (1919)
30. Theodorsen, T.: Theory of propellers. McGraw-Hill, New York (1948)
31. Wald, Q.R.: The aerodynamics of propellers. Prog. Aerosp. Sci. **42**, 85–128 (2006)
32. Okulov, V.L., Sørensen, J.N.: Refined Betz limit for rotors with a finite number of blades. Wind Energy **11**, 415–426 (2008)